

# Ultrasonic Needle Tracking with a Fibre-Optic Ultrasound Transmitter for Guidance of Minimally Invasive Fetal Surgery

Wenfeng Xia<sup>1</sup>(✉), Sacha Noimark<sup>1,2</sup>, Sebastien Ourselin<sup>1</sup>, Simeon J. West<sup>3</sup>, Malcolm C. Finlay<sup>1,4</sup>, Anna L. David<sup>5</sup>, and Adrien E. Desjardins<sup>1</sup>

<sup>1</sup> Department of Medical Physics and Biomedical Engineering,  
University College London, Gower Street, London WC1E 6BT, UK  
[wenfeng.xia@ucl.ac.uk](mailto:wenfeng.xia@ucl.ac.uk)

<sup>2</sup> Materials Chemistry Research Centre, Department of Chemistry,  
University College London, 20 Gordon Street, London WC1H 0AJ, UK

<sup>3</sup> Department of Anaesthesia, University College Hospital,  
235 Euston Road, London NW1 2BU, UK

<sup>4</sup> St Bartholomew's Hospital and Queen Mary University of London,  
Charterhouse Square, London EC1M 6BQ, UK

<sup>5</sup> Institute for Women's Health, University College London,  
86-96 Chenies Mews, London WC1E 6HX, UK

**Abstract.** Ultrasound imaging is widely used for guiding minimally invasive procedures, including fetal surgery. Visualisation of medical devices such as medical needles is critically important and it remains challenging in many clinical contexts. During in-plane insertions, a needle can have poor visibility at steep insertion angles and at large insertion depths. During out-of-plane insertions, the needle tip can have a similar ultrasonic appearance to the needle shaft when it intersects with the ultrasound imaging plane. When the needle tip is not accurately identified, it can damage critical structures, with potentially severe consequences, including loss of pregnancy. In this paper, we present a tracking system to directly visualise the needle tip with an ultrasonic beacon. The waves transmitted by the beacon were received by an external ultrasound imaging probe. Pairs of co-registered images were acquired in rapid succession with this probe: a photoacoustic image obtained with the system in receive-only mode, and a conventional B-mode ultrasound image. The beacon comprised a custom elastomeric nanocomposite coating at the distal end of an optical fibre, which was positioned within the lumen of a commercial 22 gauge needle. Delivery of pulsed light to the coating resulted in the photoacoustic generation of ultrasonic waves. The measured tracking accuracies in water in the axial and lateral dimensions were  $0.39 \pm 0.19$  mm and  $1.85 \pm 0.29$  mm, respectively. To obtain a preliminary indication of the clinical potential of this ultrasonic needle tracking system, needle insertions were performed in an *in vivo* fetal sheep model. The results demonstrate that ultrasonic needle tracking with a fibre-optic transmitter is feasible in a clinically realistic fetal surgery environment, and that it could be useful to guide minimally invasive procedures by providing accurate visualisation of the medical device tip.

# 1 Introduction

Ultrasound (US) imaging is used to guide needle insertions in many clinical contexts. This study is situated in the context of fetal medicine, in which procedures are performed to collect fetal samples for prenatal diagnosis with US-guided needle insertions including amniocentesis, chorionic villus sampling and fetal blood sampling [1,2]. Guidance is typically performed with an US imaging probe positioned on the maternal anterior abdominal wall. Here, a key challenge is accurate and efficient identification of the needle tip relative to the US image. Needle tip visibility can readily be lost during steep insertions when US waves are reflected outside the aperture of the imaging probe, and when the needle tip strays from the imaging plane. Severe complications can result from misplacement of the needle tip, which include the loss of pregnancy [2].

Ultrasonic needle tracking is a method for identifying the needle tip that involves US communication between the imaging probe and the needle. One implementation of this method involves transmissions from the imaging probe that are received by a piezoelectric US sensor integrated within the needle [3–5]. In recent studies by Xia *et al.*, sequential transmissions by individual elements of the imaging probe were received by a fibre-optic hydrophone (FOH) sensor within the needle lumen [6–9]. The sensor signals were processed using a time-reversal algorithm to obtain tracking images in which the FOH was the sole object. Each tracking image was inherently co-registered with a B-mode US image that was acquired with the same imaging probe. The hydrophone, which comprised a Fabry-Pérot cavity at the distal end of an optical fibre, was well suited for US sensing from within a needle, owing to its high bandwidth and low directionality [10,11].

In this study, we developed a reciprocal implementation of US needle tracking in which transmissions are made at the needle tip and received by the imaging probe. This implementation was previously considered by Mung *et al.* [12] using a piezoelectric US transmitter within a needle. Here, we present a system using an optical US transmitter: a nanocomposite coating at the distal end of an optical fibre to which pulsed light is delivered for generating US waves via the photoacoustic (PA) effect. This coating served as a beacon from which tracking images could be obtained with the imaging probe operated in receive-only mode. The relative tracking accuracy was evaluated with a water phantom, and an initial validation study was performed with an *in vivo* fetal sheep model.

# 2 Materials and Methods

## 2.1 Ultrasonic Tracking System

The ultrasonic tracking system comprised two components: a clinical US imaging system and a needle with an integrated beacon (Fig. 1(a)). The US imaging system was operated in research mode (SonixMDP, Analogic Ultrasound, Canada). The imaging probe (L14-5/38) had a linear transducer array of 128 transducer elements with a nominal bandwidth of 5–14 MHz. This system acquired pairs of

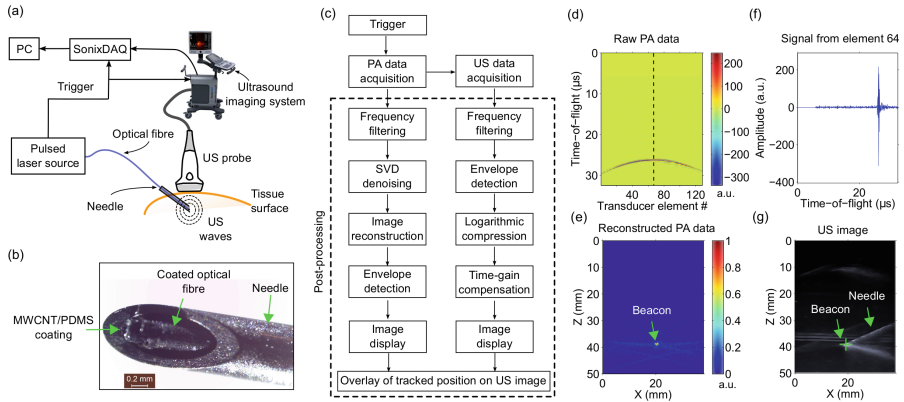


**Fig. 1.** Ultrasonic needle tracking system, shown schematically (a), with a photograph of the needle tip with the fibre-optic beacon at the distal end (b). Parallel multi-channel photoacoustic (PA) data and conventional B-mode ultrasound (US) data were acquired sequentially, and post-processed separately (c). As illustrated with acquisitions from the needle tip in water, raw PA data (d) were reconstructed to obtain a PA tracking image of the fibre-optic beacon (e; arrow). In a time series from transducer element 64, the onset of the beacon signal is apparent at  $t = 26 \mu\text{s}$  (f). The location of the beacon in the PA tracking image was coincident with that of the needle tip in the US image (g). PC: personal computer; MWCNT: multi-walled carbon nanotube; PDMS: polydimethylsiloxane; SVD: singular value decomposition; a.u.: arbitrary units.

PA and B-mode US images using the same imaging probe. For PA imaging, pre-beamformed radiofrequency (RF) data from all of the transducer elements in the imaging probe were simultaneously sampled at 40 MS/s by a multi-channel data acquisition system (SonixDAQ, Analogic Ultrasound) and transferred to the US imaging system personal computer (PC). Conventional B-mode (pulse-echo) US image acquisition was performed immediately after PA image acquisition, as detailed in [13].

The US beacon was fabricated with a custom nanocomposite coating at the end of an optical fibre. As previously described in Refs. [14,15], the coating comprised multi-walled carbon nanotubes as optical absorbers and polydimethylsiloxane (PDMS) as an elastomeric host. The coating was applied to the distal end of an optical fibre (core diameter:  $200 \mu\text{m}$ ) with dip coating. The fibre was integrated into the lumen of a 22 gauge spinal needle. It was positioned so that the coating was at the bevel surface of the needle, proximal to the sharp end and distal to the cannula (Fig. 1(b)).

Ultrasound was generated with PA excitation of the coating. Pulsed excitation light (wavelength: 1064 nm; pulse repetition rate: 30 Hz) from an Nd:YAG laser (SPOT-10-500-1064, Elforlight, UK) was delivered to the coating via the optical fibre. The pulse width was *ca.* 2 ns; the pulse energies ranged from 7.5 to  $10 \mu\text{J}$ . The laser was externally triggered with a signal that was also provided to the SonixDAQ as a PA acquisition trigger.

## 2.2 Image Processing

Processing of PA and B-mode US images was performed offline (Fig. 1(c)). For the former, the acquired RF data matrix was band-pass frequency filtered (5th order Butterworth, 5 to 14 MHz) and laser-induced noise was mitigated with singular value decomposition (SVD), as detailed in [16]. Subsequently, PA image reconstruction was performed using a Fourier domain method, implemented offline using the k-Wave MATLAB toolbox [17] with a uniform speed of sound (1480 m/s for measurements in water; 1540 m/s for measurements *in vivo*). Using a PC with a 2.93 GHz CPU (Intel Core i7-870) and 8 GB of RAM, the reconstruction time for each PA image was *ca.* 530 ms. In the RF data matrices, signals from the PA beacon were delayed according to their time-of-flights to the transducer elements (Fig. 1(d)). With the image reconstruction step, coherent summation of these signals was achieved to form an image of the beacon (Fig. 1(e)).

## 2.3 Tracking Accuracy and Signal-to-Noise Ratio Measurements

To evaluate tracking accuracy and the signal-to-noise ratio (SNR) of the PA tracking images, the imaging probe was translated relative to the beacon in deionised water. Two sets of measurements were made with distinct beacons. One beacon was bare; the other was inside the needle. Translation of the imaging probe in the depth direction was performed with a motorised stage (MTS50/M-Z8, Thorlabs, U.K.); the beacon or needle was held within the imaging plane with a mechanical mount. Across different PA tracking image acquisitions, the lateral (X) and depth (Z) coordinates of the needle tip and the angle of the optical fibre proximal to the beacon or the needle shaft ( $\theta$ , defined relative to the tissue surface) were varied. These variations took place over the ranges of 20 to 35 mm in X, 10 to 50 mm in Z, and  $26^\circ$  to  $64^\circ$  in  $\theta$ . Accuracy in the X dimension was measured as the full-width-at-half-maximum (FWHM) of the maximum intensity projection (MIP) along the Z dimension. Likewise, accuracy in the Z dimension was measured as the FWHM of the MIP along the X dimension. For SNR calculations, the signal was defined as the maximum value in a square region with a width of 5 mm and a centre coincident with the maximum value of the PA image. The noise was defined as the standard deviation of values in a non-overlapping rectangular region. For the measurements in water, this background region spanned the region of X = 0 to 15 mm and Z = 10 to 50 mm; for measurements *in vivo*, it spanned the region of X = 0 to 38 and Z = 10 to 20 mm.

## 2.4 In Vivo Validation

As a preliminary validation step, we performed ultrasonic needle tracking in a fetal sheep model *in vivo* [18]. This experiment was intended to measure the signal strength and the spatial resolution of the tracking method in a clinically realistic environment. All procedures on animals were conducted in accordance

with U.K. Home Office regulations and the Guidance for the Operation of Animals (Scientific Procedures) Act (1986). Ethics approval was provided by the joint animal studies committee of the Royal Veterinary College and the University College London, United Kingdom. The pregnant sheep was placed under general anaesthesia and monitored continuously. After cleaning of the maternal abdomen, the needle was inserted through the anterior abdominal wall and uterine myometrium, towards four target locations: the amniotic fluid, the fetal heart, the fetal umbilical vein, and a placental (a structure similar to the human placenta). In all cases, the needle bevel was facing upward. Attempts were made to maintain the needle within the imaging plane; however, as seen in clinical practice, it strayed slightly due to maternal breathing or operator movements. For each insertion, tracking was performed continuously as the optimal target location for fetal sampling (P1), which was identified on US by the practitioner (A.L.D.), was reached. Subsequently, it was performed during needle withdrawal (P2 and P3). The depths of the needle tip ranged from 23 to 42 mm.

### 3 Results and Discussion

When the beacon was in water, it was visible in all PA tracking images and in all US images. There was good agreement between the spatial locations of the beacon in both modalities. In each PA tracking image, the signals were confined to a small region surrounding the beacon. The location of the absolute maximum in this region corresponded to the location of the beacon. The axial and lateral FWHM values were similar whether or not the beacon was integrated into the needle (Fig. 2(a)–(b)). With the beacon in water, the FWHM in the axial (Z) direction ranged from 0.19 to 0.76 mm, with a mean of 0.39 mm. Likewise, the FWHM values in the lateral (X) direction ranged from 1.55 to 2.37 mm, with a mean of 1.85 mm (Fig. 2(a)). With the beacon in the needle tip, the axial and lateral FWHM values were found to be dependent on both Z, and  $\theta$ . High SNR values were observed in all cases, which ranged from 74 to 342 with a mean of 157. The SNR increased with Z by 183% over a range of 40 mm, and increased with  $\theta$  by 25% from  $26^\circ$  to  $64^\circ$  (Fig. 2(b)–(c)).

During needle insertions in the fetal sheep model *in vivo*, the beacon had a prominent appearance in all PA tracking images (Fig. 3). When the needle tip was apparent on an US image, its location was consistent with that in the corresponding PA tracking image. However, as frequently observed in clinical practice, the needle was often poorly visible with US imaging when it was in tissue. The signals in PA images were consistently confined to a small region surrounding the needle tip in all cases (Fig. 3(a)–(c)). The axial FWHM varied from 0.36 to 1.51 mm; the lateral FWHM varied from 1.91 to 3.21 mm. The SNR values ranged from 44 to 314.

In this study, tracking accuracy was defined relative to the coordinate system of the photoacoustic and ultrasound images. Depending on the spatial distortions within these images, which could arise from heterogeneities in the speed of sound, there may be differences between the relative tracking accuracy, as defined

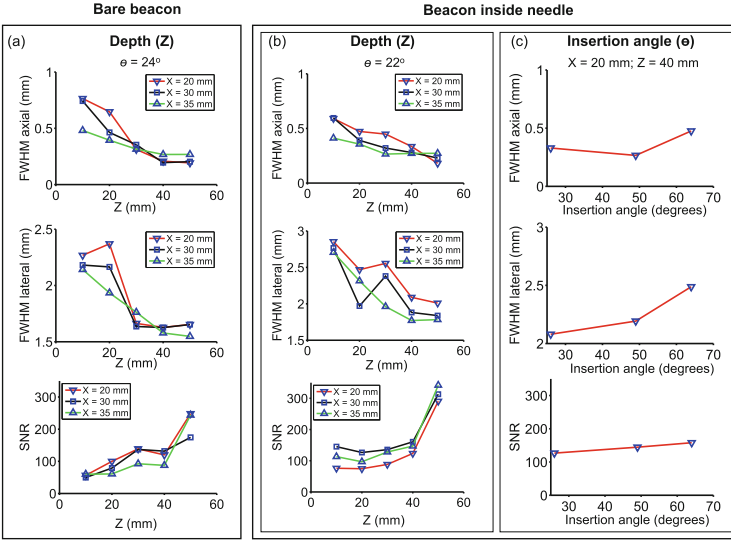


**Fig. 2.** The spatial resolution and signal-to-noise ratio (SNR) of ultrasonic tracking with the fibre-optic beacon were assessed in a water tank. Spatial resolution was measured as the full-width-at-half-maximum (FWHM) in axial and lateral directions. Two cases were considered: a bare beacon without a needle (a), and the beacon within a needle (b–c) as shown in Fig. 1(b). Insertion angle  $\theta$  was measured relative to the surface, with  $0^\circ$  corresponding to the needle parallel to the tissue surface.

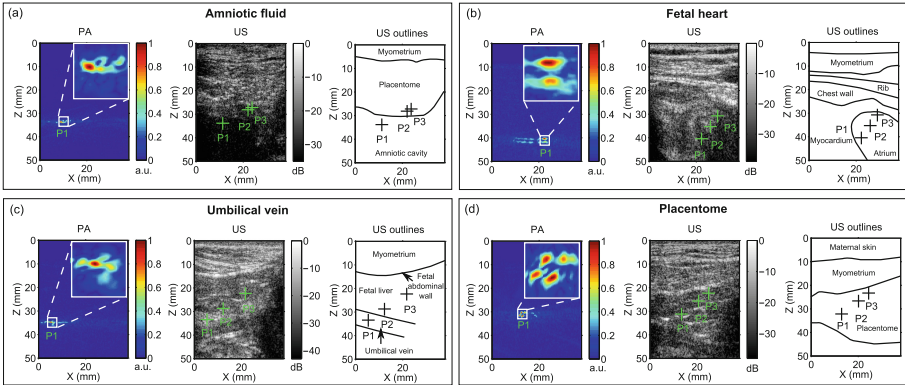


**Fig. 3.** *In vivo* validation of the ultrasonic tracking system in a fetal sheep model. Four insertions within the ultrasound (US) imaging plane are shown, in which the needle tip reached the amniotic fluid (a), the fetal heart (b), the umbilical vein (c), and a placentome (d). For each image, the photoacoustic (PA) tracking image from the optimal target position (P1) is shown, with an inset of  $4\text{ mm} \times 4\text{ mm}$ . The tracked positions derived from the PA images are overlaid on the US images, including two points (P2 and P3) attained during withdrawal.

here, and the absolute tracking accuracy, as defined relative to a coordinate system external to the patient. When the absolute positions of the needle tip and anatomical structures are unknown, as is usually the case during ultrasound-guided procedures, relative tracking accuracy is the more salient performance metric.

This study is, to the authors' knowledge, the first in which ultrasonic tracking of a medical device is performed with a beacon comprising a fibre-optic US transmitter and simultaneous reception of US across all channels of an imaging probe. A key observation made in this study is that a transmitter with a simple geometry, in which the PDMS-CNT optical absorber is applied directly to a flat-cleaved optical fibre, can generate sufficiently high amplitude transmissions in the backwards direction to enable needle tracking across a range of insertion angles that are encountered in clinical practice. With its diminutive size, this transmitter could be readily incorporated into a wide range of medical devices. Future optimisations to the transmitter could include optical absorption surfaces that are domed or extended in length to achieve different angular transmission patterns. Optical absorbing coatings that are transmissive at certain wavelengths could be used for interventional PA imaging [13, 19, 20].

The system presented here has the advantage of providing a PA tracking image that is distinct from, and co-registered with the US images, in which solely the region in the immediate vicinity of the needle tip is apparent. Its tracking accuracy was similar to that obtained with a reciprocal system in which US was transmitted by the imaging probe and received at the needle tip [6–9]. Guo *et al.* [21] presented an active beacon system in which US transmissions from an imaging probe were received with a FOH and immediately triggered a fibre-optic PA transmitter. Metallic structures within medical devices can be a source of photoacoustic ultrasound generation, and this effect has been exploited to visualise needles and brachytherapy seeds, using light delivered both externally and internally [22–25]. Ultimately, the advantages and disadvantages of different implementations of ultrasonic tracking, including those with transmission and reception of US at the needle tip, will depend up on a multitude of factors, such as the availability of trigger signals between the PA excitation laser and the US imaging system, and the image computing requirements. As demonstrated with an *in vivo* model in this study, ultrasonic tracking is a promising method for guiding interventions in fetal medicine and many other minimally invasive procedures.

**Acknowledgments.** This work was supported by an Innovative Engineering for Health award by the Wellcome Trust (No. WT101957) and the Engineering and Physical Sciences Research Council (EPSRC) (No. NS/A000027/1), by a Starting Grant from the European Research Council (ERC-2012-StG, Proposal No. 310970 MOPHIM), and by an EPSRC First Grant (No. EP/J010952/1). A.L.D. is supported by the UCL/UCLH NIHR Comprehensive Biomedical Research Centre. The authors are grateful for the technical support provided by Dr. Richard J. Colchester, Dr. Erwin J. Alles and Dr. Sandy Mosse from UCL.

## References

1. Daffos, F., et al.: Fetal blood, sampling during pregnancy with use of a needle guided by ultrasound: a study of 606 consecutive cases. *Am. J. Obstet. Gynecol.* **153**(6), 655–660 (1985)
2. Agarwal, K., et al.: Pregnancy loss after chorionic villus sampling and genetic amniocentesis in twin pregnancies: a systematic review. *Ultras. Obstet. Gynecol.* **40**(2), 128–134 (2012)
3. Breyer, B., et al.: Ultrasonically marked catheter—a method for positive echographic catheter position identification. *Med. Biol. Eng. Comput.* **22**(3), 268–271 (1984)
4. Winsberg, F., et al.: Use of an acoustic transponder for US visualization of biopsy needles. *Radiology* **180**(3), 877–878 (1991)
5. Mung, J., et al.: Ultrasonically marked instruments for ultrasound-guided interventions. In: *IEEE Ultrasonics Symposium (IUS)*, pp. 2053–2056 (2013)
6. Xia, W., et al.: In-plane ultrasonic needle tracking using a fiber-optic hydrophone. *Med. Phys.* **42**(10), 5983–5991 (2015)
7. Xia, W., et al.: Interventional photoacoustic imaging of the human placenta with ultrasonic tracking for minimally invasive fetal surgeries. In: Navab, N., Hornegger, J., Wells, W.M., Frangi, A.F. (eds.) *MICCAI 2015. LNCS*, vol. 9349, pp. 371–378. Springer, Cham (2015). doi:[10.1007/978-3-319-24553-9\\_46](https://doi.org/10.1007/978-3-319-24553-9_46)
8. Xia, W., et al.: Coded excitation ultrasonic needle tracking: an in vivo study. *Med. Phys.* **43**(7), 4065–4073 (2016)
9. Xia, W., West, S.J., Mari, J.-M., Ourselin, S., David, A.L., Desjardins, A.E.: 3D ultrasonic needle tracking with a 1.5D transducer array for guidance of fetal interventions. In: Ourselin, S., Joskowicz, L., Sabuncu, M.R., Unal, G., Wells, W. (eds.) *MICCAI 2016. LNCS*, vol. 9900, pp. 353–361. Springer, Cham (2016). doi:[10.1007/978-3-319-46720-7\\_41](https://doi.org/10.1007/978-3-319-46720-7_41)
10. Morris, P., et al.: A Fabry-Pérot fiber-optic ultrasonic hydrophone for the simultaneous measurement of temperature and acoustic pressure. *J. Acoust. Soc. Am.* **125**(6), 3611–3622 (2009)
11. Zhang, E.Z., et al.: A miniature all-optical photoacoustic imaging probe. In: *Proceedings of SPIE 7899*, pp. 78991F (2011)
12. Mung, J., et al.: Design and in vitro evaluation of a real-time catheter localization system using time of flight measurements from seven 3.5 MHz single element ultrasound transducers towards abdominal aortic aneurysm procedures. *Ultrasonics* **51**(6), 768–775 (2011)
13. Xia, W., et al.: Performance characteristics of an interventional multispectral photoacoustic imaging system for guiding minimally invasive procedures. *J. Biomed. Opt.* **20**(8), 086005 (2015)
14. Colchester, R.J., et al.: Laser-generated ultrasound with optical fibres using functionalised carbon nanotube composite coatings. *Appl. Phys. Lett.* **104**(17), 173502 (2014)
15. Noimark, S., et al.: Carbon-nanotube-PDMS composite coatings on optical fibers for all-optical ultrasound imaging. *Adv. Funct. Mater.* **26**(46), 8390–8396 (2016)
16. Hill, E.R., et al.: Identification and removal of laser-induced noise in photoacoustic imaging using singular value decomposition. *Biomed. Opt. Express* **8**(1), 275501 (2017)
17. Treeby, B.E., et al.: k-Wave: MATLAB toolbox for the simulation and reconstruction of photoacoustic wave fields. *J. Biomed. Opt.* **15**(2), 021314 (2010)



18. David, A.L., et al.: Recombinant adeno-associated virus-mediated in utero gene transfer gives therapeutic transgene expression in the sheep. *Hum. Gene Ther.* **22**, 419–426 (2010)
19. Piras, D., et al.: Photoacoustic needle: minimally invasive guidance to biopsy. *J. Biomed. Opt.* **18**(7), 070502 (2013)
20. Mari, J.M., et al.: Interventional multispectral photoacoustic imaging with a clinical ultrasound probe for discriminating nerves and tendons: an ex vivo pilot study. *J. Biomed. Opt.* **20**(11), 110503 (2015)
21. Guo, X., et al.: Active ultrasound pattern injection system (AUSPIS) for interventional tool guidance. *PLoS One* **9**(10), e104262 (2014)
22. Kang, H.J., et al.: Needle visualization using photoacoustic effect. In: *SPIE BiOS*, pp. 93232Y. International Society for Optics and Photonics (2015)
23. Su, J., et al.: Photoacoustic imaging of clinical metal needles in tissue. *J. Biomed. Opt.* **15**(2), 021309 (2010)
24. Wei, C.W., et al.: Clinically translatable ultrasound/photoacoustic imaging for real-time needle biopsy guidance. In: *IEEE International Ultrasonics Symposium (IUS)*, pp. 839–842 (2014)
25. Singh, M.K.A., et al.: Photoacoustic-guided focused ultrasound for accurate visualization of brachytherapy seeds with the photoacoustic needle. *J. Biomed. Opt.* **21**(12), 120501 (2016)